

# Adaptive neuro-fuzzy approach to predict tool wear accurately in turning operations for maximum cutting tool utilization

Ahmed A. D. Sarhan

*Advanced Manufacturing and Material Processing Centre, Department of Mechanical Engineering, Faculty of Engineering,  
University of Malaya, 50603, Kuala Lumpur*

*(Tel: 0060379674593; e-mail: [ah\\_sarhan@um.edu.my](mailto:ah_sarhan@um.edu.my))*

**Abstract:** In industry, the capability to predict tool wear is an essential matter as the quality and performance of a cutting tool directly affect the product quality. Developing a model to predict tool wear can help control tool wear and maximize tool utilization. Therefore, this study presents a method of predicting tool flank wear of coated carbide inserts while machining AISI 1050 low carbon steel with a turning operation. The adaptive neuro-fuzzy approach (ANFIS) was implemented in this research. Experiments were conducted based on the Design of Experiments (DOE) technique by developing experiments with four factors at four levels corresponding to the  $L_{16}$  ( $4^4$ ) experimental array to measure tool flank wear. At the end, a verification test was conducted to illustrate the effectiveness of this approach. Using ANFIS, average prediction accuracy of 92.42% was obtained and the ANFIS tool wear model developed indicated how the interaction between factors influenced tool wear.

© 2015, IFAC (International Federation of Automatic Control) Hosting by Elsevier Ltd. All rights reserved.

**Keywords:** Tool flank wear prediction, AISI 1050 low carbon steel, coated carbide insert, ANFIS approach, turning operation

## 1. INTRODUCTION

Turning is a common machining process used especially for the finishing of components. In machining, tool wear is a natural phenomenon that refers to the cutting tool gradually losing its cutting ability, progressively leading to tool failure [1]. Tool wear is definitely unpleasant because as it increases to a certain value, the tool needs to be changed. Replacement with a new tool results in process interruption and rising machining cost, which is the most undesirable consequence in the manufacturing field. Therefore, to achieve high quality machining performance, machining parameter selection and control are essential. Several methods used in the selection of optimum cutting conditions are based on the operator's experience or a design data book [2]. The conventional method of determining the optimal values is the "trial and error" approach. However, due to the large number of experiments, "trial and error" is very time consuming. Hence, a reliable, systematic approach to optimizing parameters is required. Therefore, mathematical and scientific approaches have been designed and developed for selecting machining parameters and predicting the behaviour of machining performance. The presence of prediction models should eliminate unnecessary cost and time-consuming trial and error methods to find stable cutting conditions. Soft computing techniques are often selected as prediction models due to their effectiveness and simplicity. Such

methods are useful when exact mathematical information is not available, and these differ from conventional computing in that they are tolerant to imprecision, uncertainty, partial truth, approximation, and met heuristics [3, 4]. ANFIS is among the soft computing techniques that play a significant role in modeling input-output matrix relationships. It is used when subjective knowledge and expert suggestions are substantial to defining the objective function and decision variables. ANFIS is ideal for predicting tool wear based on input variables due to the nonlinear condition in the machining process [5-9].

As a conclusion of the above review, the aim of the present work is to develop an accurate prediction model of tool wear using the ANFIS modeling technique for maximum cutting tool utilization.

## 2. METHODOLOGY

### 2.1 Design of Experiment

Parameter design was implemented in this study because it is recognized as able to significantly reduce the number of experiments. The  $L_{16}$  experimental array, as shown in Table 1, was used for its four factors, and each was identified at four levels as the input variables. The factors and their levels are presented in Table 2. The parameter range was selected based on the tool manufacturer's recommendation.

**Table 1. L<sub>16</sub> Experimental array and measured tool wear**

| Ex. | Cutting parameter level |    |    |    | Tool wear (μm) |
|-----|-------------------------|----|----|----|----------------|
|     | P1                      | P2 | P3 | P4 |                |
| 1   | 1                       | 1  | 1  | 1  | 27.22          |
| 2   | 1                       | 2  | 2  | 2  | 18.33          |
| 3   | 1                       | 3  | 3  | 3  | 65.75          |
| 4   | 1                       | 4  | 4  | 4  | 38.33          |
| 5   | 2                       | 1  | 2  | 3  | 67.78          |
| 6   | 2                       | 2  | 1  | 4  | 18.33          |
| 7   | 2                       | 3  | 4  | 1  | 30.56          |
| 8   | 2                       | 4  | 3  | 2  | 40.22          |
| 9   | 3                       | 1  | 3  | 4  | 18.89          |
| 10  | 3                       | 2  | 4  | 3  | 77.54          |
| 11  | 3                       | 3  | 1  | 2  | 21.67          |
| 12  | 3                       | 4  | 2  | 1  | 41.67          |
| 13  | 4                       | 1  | 4  | 2  | 125.56         |
| 14  | 4                       | 2  | 3  | 1  | 33.33          |
| 15  | 4                       | 3  | 2  | 4  | 18.89          |
| 16  | 4                       | 4  | 1  | 3  | 54.43          |

**Table 2. Factors and levels used in the experiment**

| Control factors |                     | Experimental condition levels |       |      |                   |
|-----------------|---------------------|-------------------------------|-------|------|-------------------|
|                 |                     | 1                             | 2     | 3    | 4                 |
| P1              | Cutting speed (rpm) | 1625                          | 1750  | 1875 | 2000              |
| P2              | Feed rate (mm/rev)  | 0.05                          | 0.1   | 0.15 | 0.2               |
| P3              | Depth of cut (mm)   | 0.5                           | 0.75  | 1    | 1.25              |
| P4              | Lubrication         | dry                           | flood | MQL  | MQL+nanolubricant |

## 2.2 Experiment Setup and Procedure

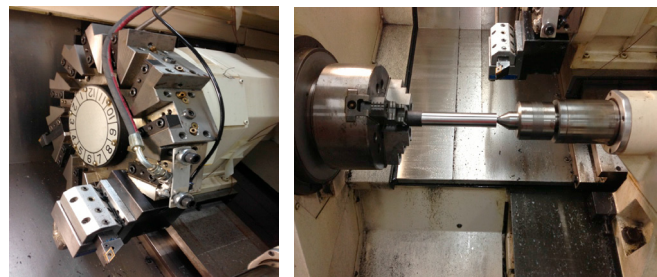
The experimental setup is shown in Fig. 1. The 16 experiments were conducted based on the experimental array. The machine used in this study was an Okuma LB15 II CNC lathe machine. The lubrication system was implemented accordingly based on the lubrication mode used in each experiment as stated in the array. Dry cutting was performed under a cooling system or air blow condition. The second mode was flood cutting, which was done using soluble cutting fluid Mobilcut 100, manufactured by Mobil. It is a conventional milky soluble oil, which forms a stable emulsion when mixed with water. The cutting fluid was obtained by mixing oil in water at a ratio of 1:20 oil to water as recommended by the manufacturer. The third lubrication mode was the MQL mode. This cutting condition was implemented using a developed cutting fluid delivery system. The delivery system parameters were set at 400 pulse/min pulsing rate, 20 Mpa air pressure and 10 ml/h delivery rate. The nozzle was attached to a flexible holder to allow adjusting the orientation of cutting fluid delivery for efficient fluid delivery. The nozzle was fixed at the tool turret to ensure continuous cutting fluid delivery to the cutting point throughout the whole cutting process. The oil used in MQL was ECOCUT SSN 332, produced by FUCHS. The last lubrication mode was nanolubricant. It uses the exact same cutting fluid delivery system, setup and delivery parameters as the MQL lubrication mode mentioned previously. The major difference is the cutting fluid used. Nanolubricant was prepared by dispersing nanopowder into cutting oil (ECOCUT SSN 332). The nanopowder was Silicon Dioxide (SiO<sub>2</sub>) of 5-15 nm size under the BET testing method with 99.5% metal basis.

Table 3 shows the properties of Silicon Dioxide. Because the average particles size of Silicon Dioxide is 5-15 nanometres, the concentration of nanopowder added was 1% of the weight of the cutting oil used, as obtained from one of our previous research works [10]. The cutting oil and Silicon Dioxide were first stirred into a mixture using a hotplate magnetic stirrer, which employs a rotating magnetic field that causes the stir bar to spin very quickly. After that, the solution was placed in an ultrasonic vibration bath for 4 hours to attain effective nanoparticle dispersion. The ultrasonic energy in this device served to break up the nanoparticle aggregates suspended in the solution.

The tool used throughout the study was a coated carbide insert confirmed to ISO designation DNMG150608. The workpiece was an AISI 1050 low carbon steel round rod with a diameter of 32 mm and length of 200 mm. The oxidized layer of the workpiece was removed by cutting 0.25 mm of the material prior to the experiment. A preliminary study on the tool wear behaviour of the selected tool was carried out before conducting the experiment to understand the behaviour of tool wear. The experiment to obtain the tool wear curve was done under fixed cutting conditions and dry cutting mode. The cutting speed, feed and depth of cut were 1900 rpm, 0.20 mm/rev and 1.00 mm, respectively, for every experimental run. The time for each run was recorded and the tool flank wear was measured after each run with a Somotech Microscope. A curve of average tool flank wear against time was plotted to observe the wear rate.



(a) CNC Lathe Machine Type Okuma LB15 II



(b) Tool, workpiece and lubrication mode setting

**Fig. 1. Experiment Setup**

**Table 3. Properties of silicon dioxide Nanopowder**

| Properties       | Description              |
|------------------|--------------------------|
| Purity           | 99.50%                   |
| APS              | 15-20nm                  |
| SSA              | 170-200m <sup>2</sup> /g |
| Colour           | White                    |
| Bulk Density     | <0.10g/cm <sup>3</sup>   |
| True Density     | 2.4g/cm <sup>3</sup>     |
| Refractive index | 1.46                     |

### 3. EXPERIMENTAL RESULTS

Figure 2 shows the tool life curve of a coated carbide insert for machining AISI 1050 low carbon steel in dry cutting mode, 1900 rpm cutting speed, 0.20 mm/rev feed rate and 1.00 mm depth of cut. The curve indicates the relationship between the average tool flank wear with accumulating cutting time. According to the ISO standard, flank wear is measured by the width of the flank wear area, VB, shown schematically in Fig. 3.

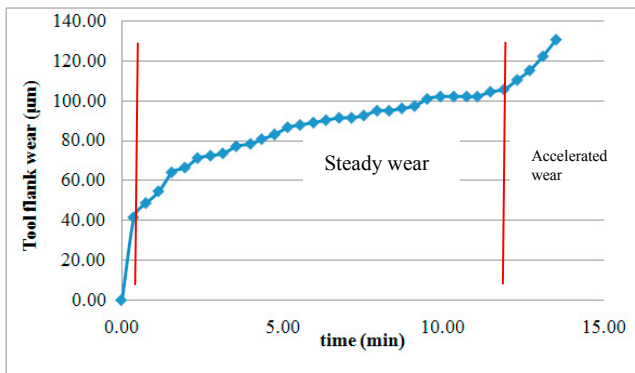


Fig. 2. Tool life curve of coated carbide insert for machining of AISI 1050 in dry cutting mode, 1900 rpm cutting speed, 0.20 mm/rev feed rate and 1.00 mm depth of cut

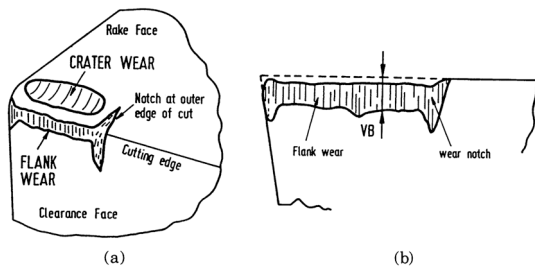


Fig. 3. (a) Regions of tool wear on a cutting tool; (b) measurement of flank wear [1]

The tool life curve can be divided into three stages: break-in wear stage at the onset when the tool wear rate is faster and occurs over a very short time period, and it ends after 0.38 min for average tool flank wear of 42 μm. The second stage is steady state wear, when the tool wear rate is slow and steady. The last stage is the accelerating tool wear stage, when wear accelerates rapidly, followed by tool failure. It starts at average tool flank wear of 115.47 μm and continues

until the end of the tool life. N.R. Dhar et al. (2006) stated that the rapid tool rate at the break-in wear stage is caused by attrition and microchipping at the sharp cutting edges [11]. In order to obtain fair results and avoid the influence of unsteady wear in the running-in stage, machining was started with a new, sharp insert that was initially worn to a steady-state wear level (45-60 μm average tool flank value). Due to the initial wear being unstable, cutting the same amount of material did not ensure a constant amount of tool wear. Therefore, for subsequent experiments, the net average tool flank wear values were taken as the tool wear values by taking the difference of the final average and initial average tool flank wear.

Tool wear was measured at three specific points for every experiment. The measured net average tool flank wear obtained in the 16 experiments are summarized in Table 2. In addition, standard deviation was applied to verify the relevance of the measured tool wear. Standard deviation (STD) can be calculated using the following equation:

$$STD = \sqrt{\frac{\sum(X_i - \mu)^2}{N}}$$

Where X = measured tool wear;

i = point no.;

μ = mean of tool wear;

N = no. of measurements.

According to Chebyshev's theorem on standard deviation (STD), low STD values indicate the data is close to the mean and large STD values signify scattering. The theorem states that at least 75% of data must lie between  $\mu \pm 2\sigma$ . Therefore, in this study, five samples from the 16 experiments were selected to determine the STD. The results indicate that the tool flank wear measured at 3 different points were relevant as shown in Table 4.

**Table 4. Standard Deviation**

| Ex. No. | Tool wear (μm) | σ    | μ ± 2σ |
|---------|----------------|------|--------|
| 1       | 80.0           | 10.8 | 100    |
| 4       | 98.3           | 16.5 | 100    |
| 8       | 83.3           | 11.8 | 100    |
| 12      | 95.0           | 12.3 | 100    |
| 16      | 113.3          | 9.4  | 100    |

### 4. ANFIS MODELLING

The measured tool wear values in Table 2 were used as the training dataset to build the ANFIS model. Five network layers were used by ANFIS to perform the following fuzzy inference steps (Fig. 4): Layer 1 - input fuzzification; Layer 2 - fuzzy set database construction; Layer 3 - fuzzy rule base construction; Layer 4 - decision making; and Layer 5 - output de-fuzzification [3-5].

To explain this model, two rules and two linguistic values for each input variable are suggested.

**Layer 1:** the output of the node is the degree to which the given input satisfies the linguistic label associated with this



node. Usually, bell-shaped membership functions are chosen to represent the linguistic terms because the relationship between the cutting parameters and surface roughness is not linear.

First parameter membership function:

$$A_i(x) = \exp[-0.5((x-a_{i1})/b_{i1})^2] \quad (1)$$

Second parameter membership function:

$$B_i(y) = \exp[-0.5((y-a_{i2})/b_{i2})^2] \quad (2)$$

Third parameter membership function:

$$C_i(u) = \exp[-0.5((u-a_{i3})/b_{i3})^2] \quad (3)$$

Fourth parameter membership function:

$$D_i(v) = \exp[-0.5((v-a_{i4})/b_{i4})^2] \quad (4)$$

where  $a_{i1}$  to  $a_{i4}$ ,  $b_{i1}$  to  $b_{i4}$  are the parameter sets.

As the values of these parameters change, the bell-shaped functions vary accordingly, thus exhibiting various forms of membership functions on linguistic labels  $A_i$ ,  $B_i$ ,  $C_i$ , and  $D_i$ . The parameters in this layer are referred to as principle parameters.

**Layer 2:** each node computes the firing strength of the associated rule. The nodes of this layer are called rule nodes. The outputs of the top and bottom neurons are as follows:

$$\text{Top neuron} \quad w_1 = A_1(x) \times B_1(y) \times C_1(u) \times D_1(v) \quad (5)$$

$$\text{Second neuron} \quad w_2 = A_1(x) \times B_1(y) \times C_1(u) \times D_2(v) \quad (6)$$

$$\vdots \quad \vdots \quad \vdots \quad \vdots \quad \vdots$$

$$\text{Bottom neuron} \quad w_n = A_n(x) \times B_n(y) \times C_n(u) \times D_n(v) \quad (7)$$

**Layer 3:** every node in this layer is labelled with N to indicate the normalization of the firing levels. The output of the top and bottom neurons is normalized as follows:

$$\text{Top neuron} \quad \bar{w}_1 = w_1 / (w_1 + w_2 + \dots + w_n) \quad (8)$$

$$\text{Second neuron} \quad \bar{w}_2 = w_2 / (w_1 + w_2 + \dots + w_n) \quad (9)$$

$$\vdots \quad \vdots \quad \vdots \quad \vdots \quad \vdots$$

$$\text{Bottom neuron} \quad \bar{w}_n = w_n / (w_1 + w_2 + \dots + w_n) \quad (10)$$

**Layer 4:** the output of the top and bottom neurons is the product of the normalized firing level and the individual rule output of the first rule and second rule respectively.

$$\text{Top neuron} \quad \bar{w}_1 z_1 = \bar{w}_1 (a_1 x + b_1 y + c_1 u + d_1 v) \quad (11)$$

$$\text{Second neuron} \quad \bar{w}_2 z_2 = \bar{w}_2 (a_2 x + b_2 y + c_2 u + d_2 v) \quad (12)$$

$$\vdots \quad \vdots \quad \vdots \quad \vdots \quad \vdots$$

$$\text{Bottom neuron} \quad \bar{w}_n z_n = \bar{w}_n (a_n x + b_n y + c_n u + d_n v) \quad (13)$$

**Layer 5:** the single node in this layer computes the overall system output as the sum of all incoming signals, i.e.

$$z = \bar{w}_1 z_1 + \bar{w}_2 z_2 + \dots + \bar{w}_n z_n \quad (14)$$

If a crisp training set  $\{(x^k, y^k, u^k, v^k) \mid k = 1, \dots, k\}$  is given, then the parameters of the hybrid neural net (which determine the shape of the membership functions of the premises) can be learned by descent-type means. The error function for pattern  $k$  is given by:

$$E_k = (o^k - z^k)^2 \quad (15)$$

where  $o^k$  is the desired output and  $z^k$  is the output computed by the hybrid neural net [5].

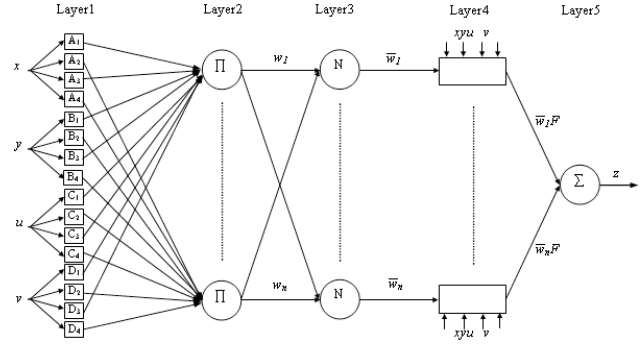


Fig. 4 ANFIS architecture for a Sugeno fuzzy model

## 5. ANFIS PREDICTION MODEL RESULTS

Surface models with two parameters showing two-way interactions and relations toward the output response of tool wear, were constructed and simulated using MATLAB software. These models not only show the effect of two machining parameters on machining performance but also give the output value in numerical form.

Figures 5 (a - c) represent the ANFIS surface models of tool wear for different combinations of machining parameters. Depth of cut appears to have significant effect on tool wear. Machining at high depth of cut shortened the tool life. In other words, at lower depth of cut, minimal tool wear was obtained. The interaction between cutting speed and feed rate shows that using high cutting speed and high feed rate increased the tool wear. The interaction between cutting speed and depth of cut indicated that at lower depth of cut, cutting speed did not have significant effect on tool wear. However, at higher depth of cut, cutting speed significantly affected the tool wear. Using higher cutting speed and depth of cut resulted in high tool wear. The interaction between feed rate and lubrication mode shows that applying lubrication had no significant effect on reducing the tool wear at lower feed rate values. However, at higher feed rates, the lubrication mode had significant effect on reducing the tool wear. At high feed rate, MQL in nanolubrication condition exhibited the lowest tool wear compared to other lubrication modes.

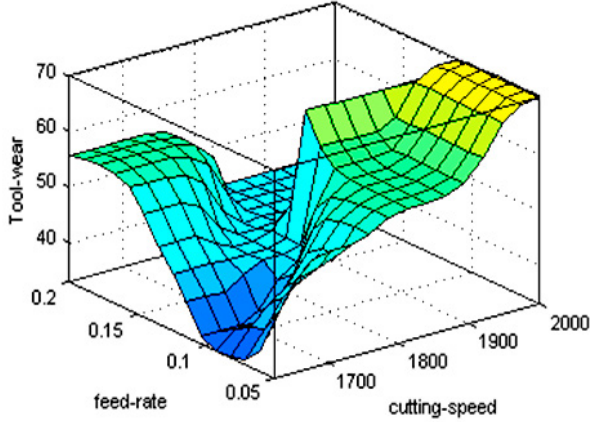
To investigate the ANFIS model accuracy and error, three new experimental tests were carried out, while the proposed ANFIS model was used to predict tool wear in the same conditions as shown in Table 5. The individual error percentage was obtained by dividing the absolute difference of the predicted and measured values by the measured value,

as given in Equation (11), where  $e_i$  is individual error,  $V_m$  is the measured value and  $V_p$  is the predicted value [4].

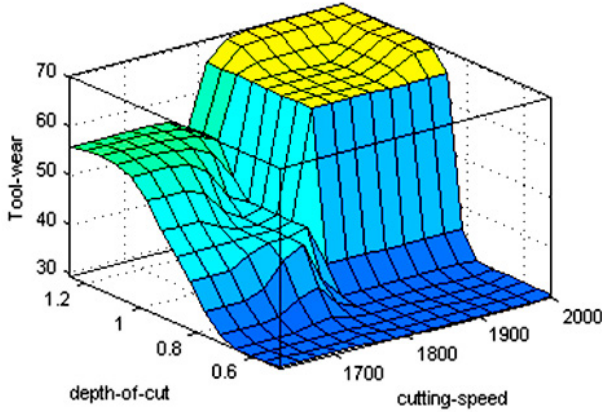
$$e_i = \left( \frac{|H_m - H_p|}{H_m} \right) \times 100\% \quad (16)$$

model accuracy is the average of individual accuracy as seen in Equation (12), where  $A$  is the model accuracy and  $N$  is the total number of data sets tested.

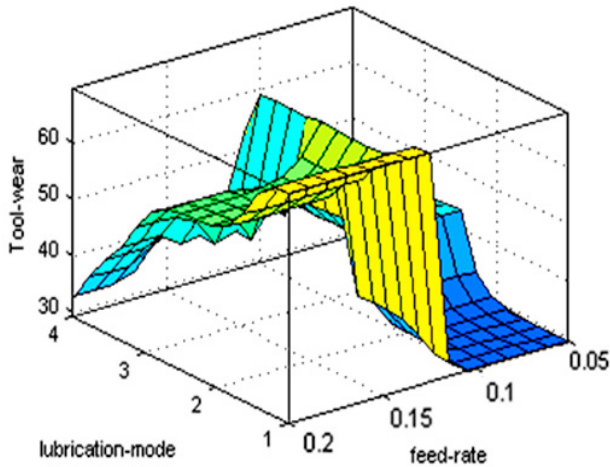
$$A = \frac{1}{N} \sum_{i=1}^N \left[ \left( 1 - \frac{|H_m - H_p|}{H_m} \right) \right] \times 100\% \quad (17)$$



(a) Interaction between cutting speed and feed rate



(b) Interaction between cutting speed and depth of cut



(c) Interaction between feed rate and lubrication mode

Fig. 5. The ANFIS surface models for tool wear at different machining parameter combinations

Meanwhile, accuracy was calculated to measure the closeness of the predicted value to the measured value. The

The error for the dataset result was calculated and the ANFIS model accuracy was determined (Table 5). The highest percentage of error for ANFIS model prediction was 6.91%. The low error level indicates that the tool wear results predicted by ANFIS were very close with the actual experimental values. Table 5 also shows that the ANFIS model accuracy was 94.8%. This signifies that the proposed model can predict tool wear satisfactorily (Fig 6).

**Table 5. Accuracy and error of ANFIS model tool wear prediction**

| Test No. | Level of cutting parameters |    |    |    | Measured tool wear ( $\mu\text{m}$ ) | Predicted tool wear ( $\mu\text{m}$ ) | Error % | Accuracy % |
|----------|-----------------------------|----|----|----|--------------------------------------|---------------------------------------|---------|------------|
|          | P1                          | P2 | P3 | P4 |                                      |                                       |         |            |
| 1        | 1                           | 1  | 1  | 1  | 27.22                                | 29.10                                 | 6.91    | 93.09      |
| 2        | 2                           | 4  | 3  | 2  | 40.22                                | 42.93                                 | 6.74    | 93.26      |
| 3        | 3                           | 2  | 4  | 3  | 77.54                                | 73.5                                  | 5.21    | 94.8       |

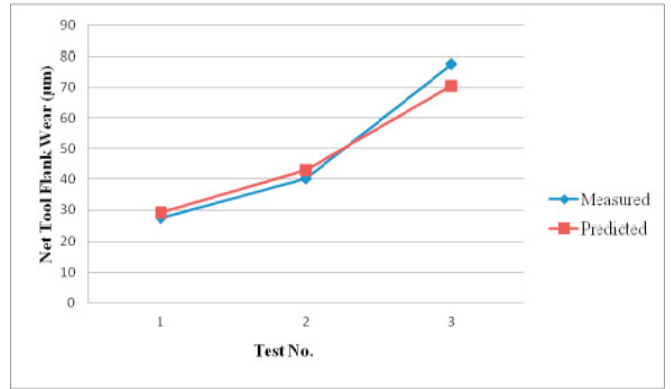


Fig. 6. Measured and Predicted Tool Wear

## 6. DISCUSSION

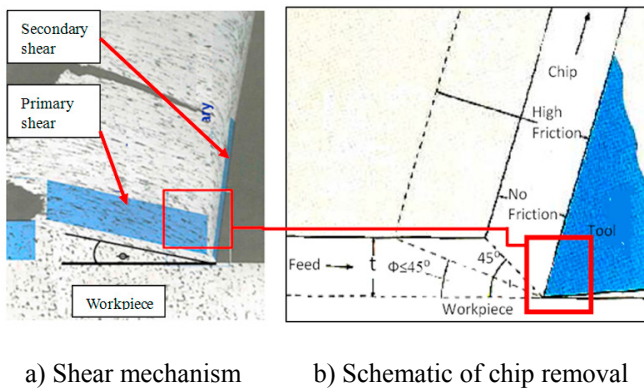
From the results, it is clear that using MQL + SiO<sub>2</sub> nanolubrication produces the lowest tool wear. This can be explained by Figs. 7 and 8 and the fact that chip deformation flows over the tool, leading to localized regions of intense shear due to the friction at the rake face (known as secondary shear). A coefficient of friction greater than 0.5 will result in a higher frictional force component  $F_f$ , leading to sticky friction. Then chip flow will occur only within the workpiece and not at the tool-workpiece interface. Consequently, the deformed chip thickness will increase, leading to a decrease in cutting ratio and shear angle  $\Phi$  and increase in shear length. Hence, the cutting force  $F_c$  component required to remove the chips will increase significantly, and consequently, tool wear will increase as well (Fig. 8) [11]. Furthermore, at higher plastic deformation, the chips are welded to the tool face, hence, effectively changing the tool geometry and rake steepness. This results in higher tool wear rate as the bits of the welded chip will eventually break off. These bits tend to be problematic due to the very hard and abrasive work hardening they undergo.

Applying the lubrication system to the tool-chip interface will reduce the coefficient of friction, leading to less cutting force and tool wear. However, introducing the  $\text{SiO}_2$  nanolubrication system would show much less friction as well as tool wear. This would mainly be attributed to the tribological properties of the  $\text{SiO}_2$  nanoparticles, which reduce the coefficient of friction at the tool-chip interface during machining as they act as billions of nano-scale quasi-spherical structured rolling elements (Fig. 11). Additionally, it is believed that the cutting zone temperature will decline as well and result in less tool wear.

## 7. CONCLUSION

This research work was aimed at developing an accurate model for predicting tool wear using ANFIS modelling for maximum cutting tool utilization. The following conclusions can be drawn based on the experimental results of the study:

1. ANFIS modelling is an adept technique for tool wear prediction with low error and high accuracy levels of 6.91 and 94.8% respectively.
2. High cutting speed and high feed rate increase tool wear.
3. At lower depth of cut, cutting speed effect on tool wear is not significant. However, at higher depth of cut, cutting speed significantly affects tool wear.
4. Using MQL with  $\text{SiO}_2$  nanolubrication, produces the lowest tool wear compared to other lubrication modes.



a) Shear mechanism      b) Schematic of chip removal

Fig. 7 Schematic of chip removal and shear mechanism in the cutting zone [11]

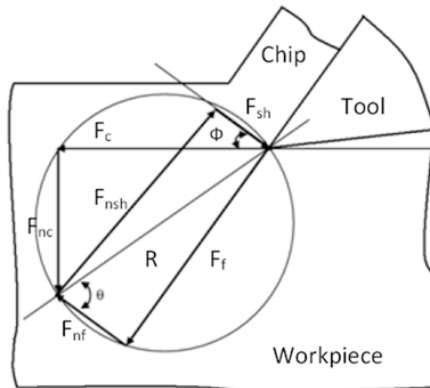


Fig. 8 Cutting mechanism [11]

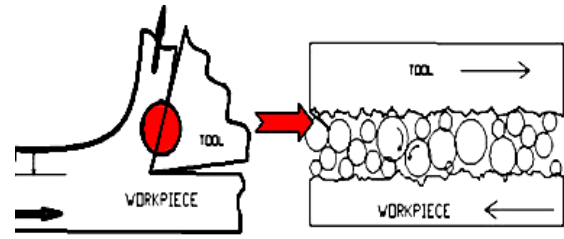


Fig. 9 Rolling elements in the tool-chip interface [10]

## ACKNOWLEDGEMENTS

This research was funded by the University of Malaya Research Grant (UMRG) Program No RP001C-13AET.

## References

- [1] B. Li (2012). A review of tool wear estimation using theoretical analysis and numerical simulation technologies. *Journal of Refractory Metals and Hard Materials* 35, 143–151.
- [2] M. Anthony Xavier, & M. Adithan (2009). Determining the influence of cutting fluids on tool wear and surface roughness during turning of AISI 304 austenitic stainless steel. *Journal of materials processing technology*, 209, 900–909.
- [3] Szecsi T (1999) Cutting force modeling using artificial neural networks. *Journal of Materials Processing Technology* 92–93 (0):344–349.  
doi:http://dx.doi.org/10.1016/S0924-0136(99)00183-1
- [4] Zalnezhad E, Sarhan AAD, Hamdi M (2013) A fuzzy logic based model to predict surface hardness of thin film TiN coating on aerospace AL7075-T6 alloy. *Int J Adv Manuf Technol* 68 (1-4):415–423. doi:10.1007/s00170-013-4738-y
- [5] Kumanan S, Jesuthanam CP, Ashok Kumar R (2008) Application of multiple regression and adaptive neuro fuzzy inference system for the prediction of surface roughness. *Int J Adv Manuf Technol* 35 (7-8):778–788. doi:10.1007/s00170-006-0755-4
- [6] Chang C-K, Lu HS (2006) Study on the prediction model of surface roughness for side milling operations. *Int J Adv Manuf Technol* 29 (9-10):867–878. doi:10.1007/s00170-005-2604-2
- [7] Kirby ED, Chen JC, Zhang JZ (2006) Development of a fuzzy-nets-based in-process surface roughness adaptive control system in turning operations. *Expert Systems with Applications* 30 (4):592–604.  
doi:http://dx.doi.org/10.1016/j.eswa.2005.07.005
- [8] Upadhyay V, Jain PK, Mehta NK (2013) In-process prediction of surface roughness in turning of Ti-6Al-4V alloy using cutting parameters and vibration signals. *Measurement* 46 (1):154–160.  
doi:http://dx.doi.org/10.1016/j.measurement.2012.06.002
- [9] Maher I, Eltaib MEH, Sarhan AD, El-Zahry RM (2014) Investigation of the effect of machining parameters on the surface quality of machined brass (60/40) in CNC end milling—ANFIS modeling. *Int J Adv Manuf Technol*:1–7. doi:http://dx.doi.org/10.1007/s00170-014-6016-z
- [10] M. Sayuti, Ahmed A. D. Sarhan, M. Hamdi, “An investigation of optimum  $\text{SiO}_2$  nanolubrication parameters in end milling of aerospace Al6061-T6 alloy”, *International Journal of Advanced Manufacturing Technology*, July 2013, V(67), Issue 1-4, pp 833-849
- [11] N.R. Dhar, M. Kamruzzaman, Mahiuddin Ahmed (2001). Effect of minimum quantity lubrication (MQL) on tool wear and surface roughness in turning AISI-4340 steel. *Journal of Materials Processing Technology*, 172, 299–304.